Electronic Supplementary Material (ESI) for RSC Advances.

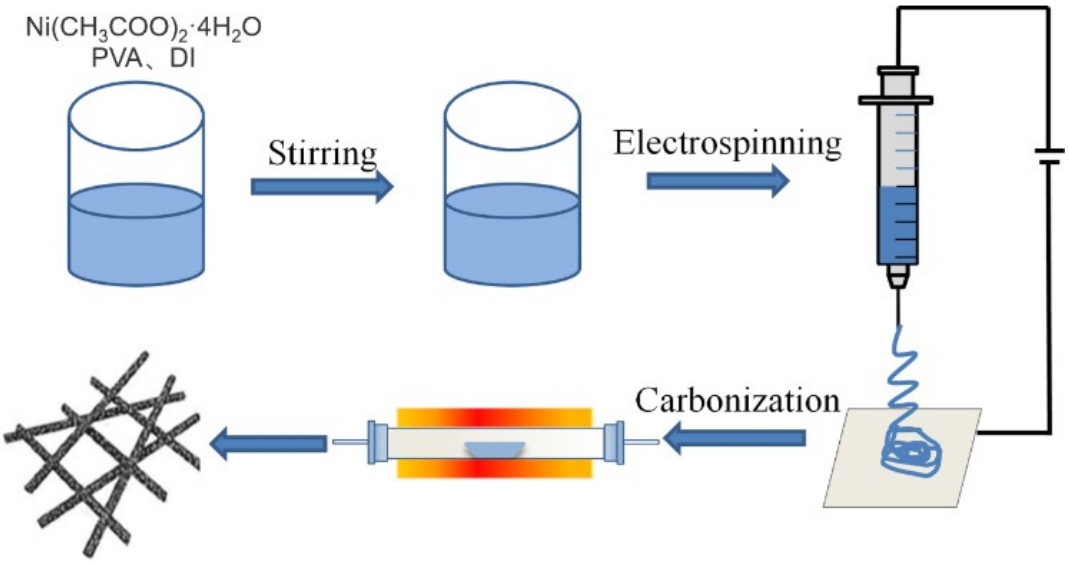

Fig.1 Sketch map of manufacture procedure of Ni/C nanofibers

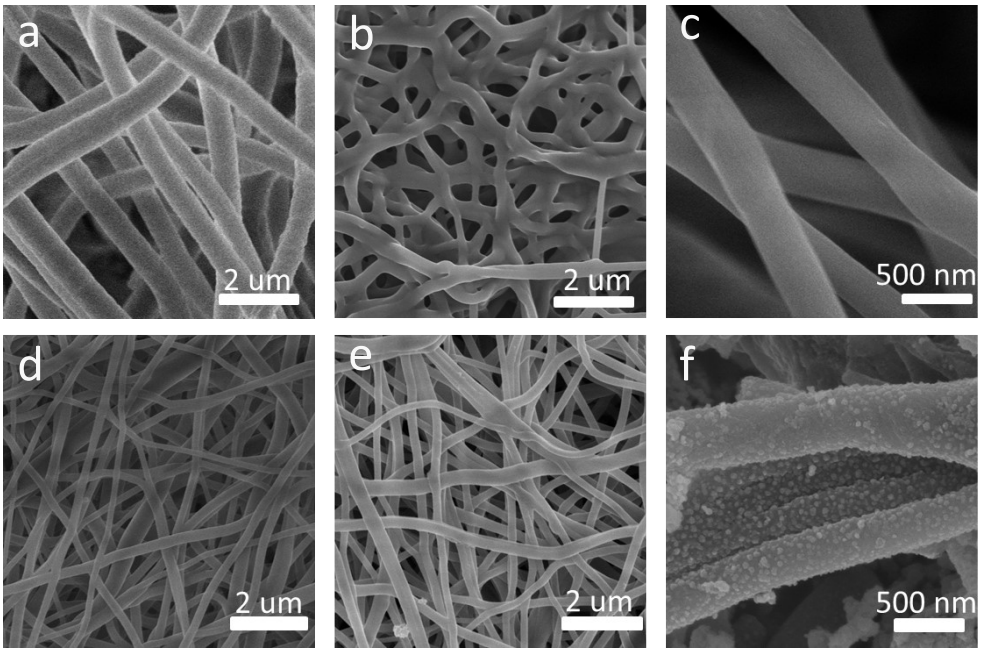

Fig. 2 SEM images of pure PVA fibers (a); Carbon nanofibers carbonized at 600℃ for 2 h (b and c); Uncarbonized Ni /PVA-based fibres (d); Ni /C nanofibers carbonized at 600℃ for 2 h (e and f)

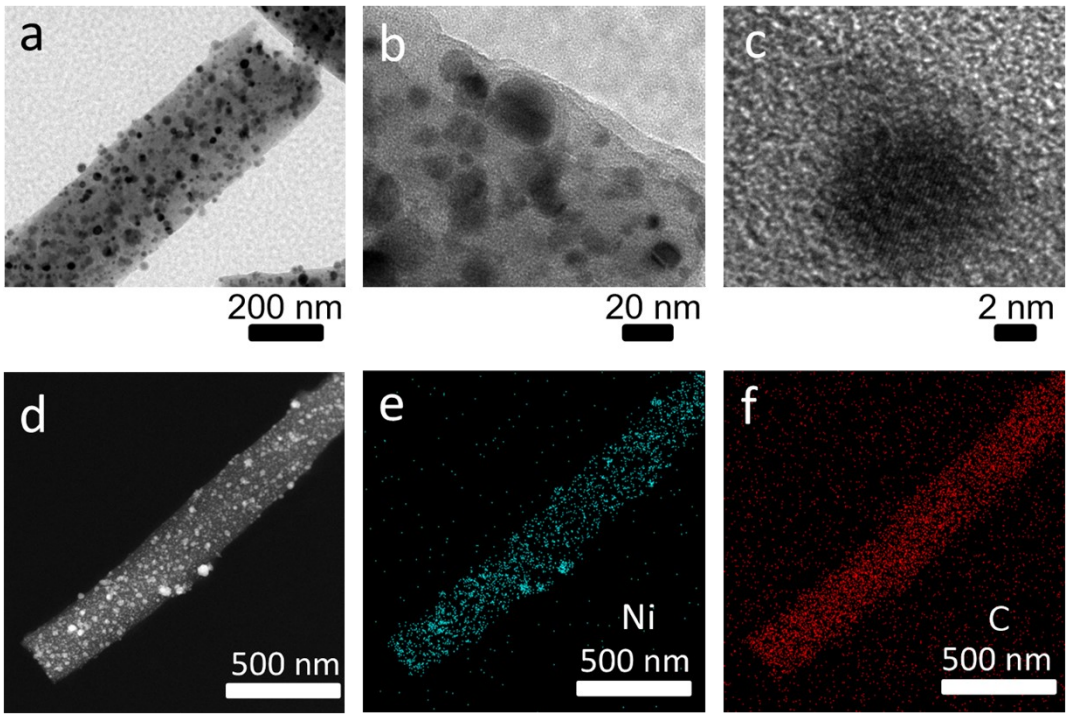

Fig. 3 TEM images of Ni /C nanofibers (a, b and c); Elemental mapping images of fibrous nano-Ni /C composites (d, e and f)

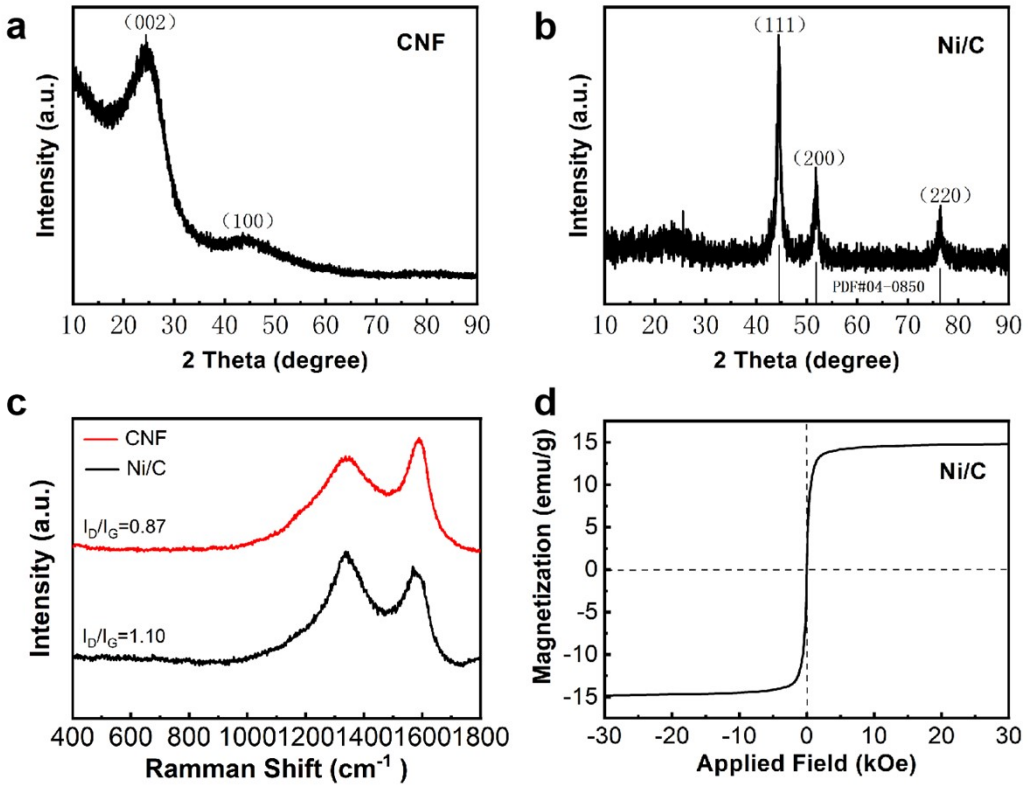

Fig. 4 XRD image of carbon nanofibers (a); XRD image (b), raman spectra (c) and hysteresis loops (d) of Ni/C nanofibers

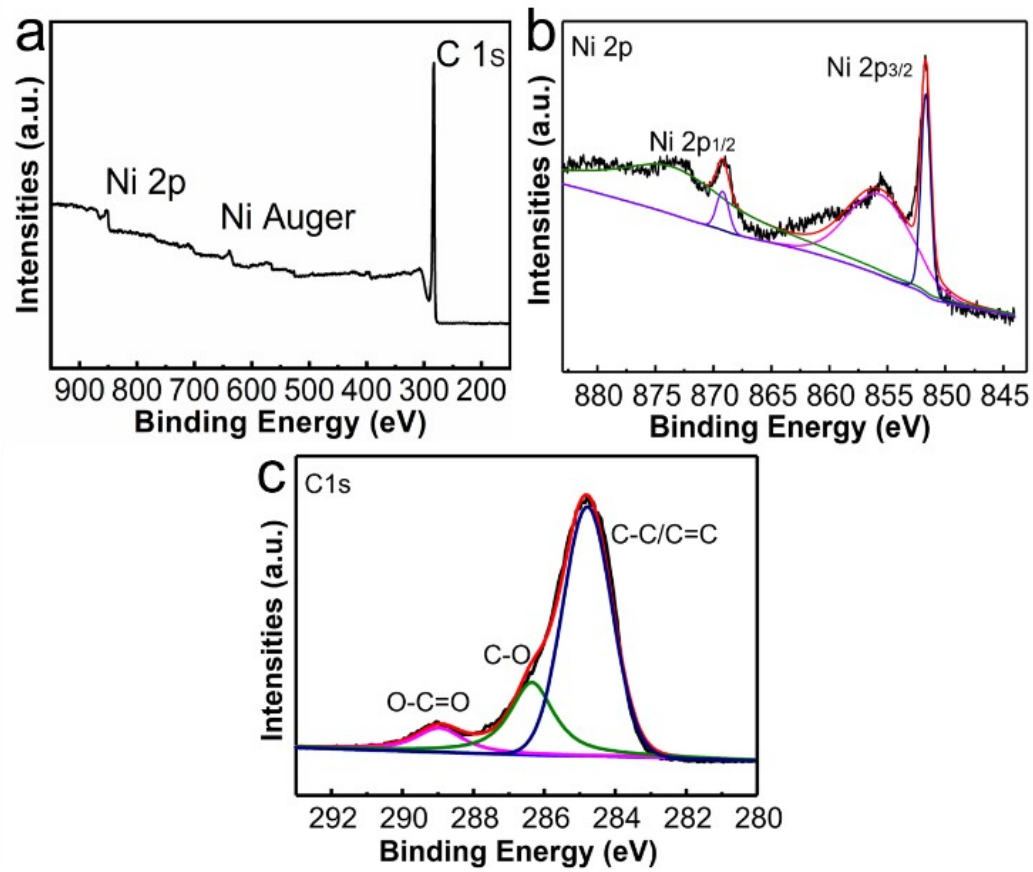

Fig. 5 XPS spectra of Ni/C nanofibers: The survey scans (a), Ni 2p spectrum (b) and C 1s spectrum (c) of Ni/C nanofibers

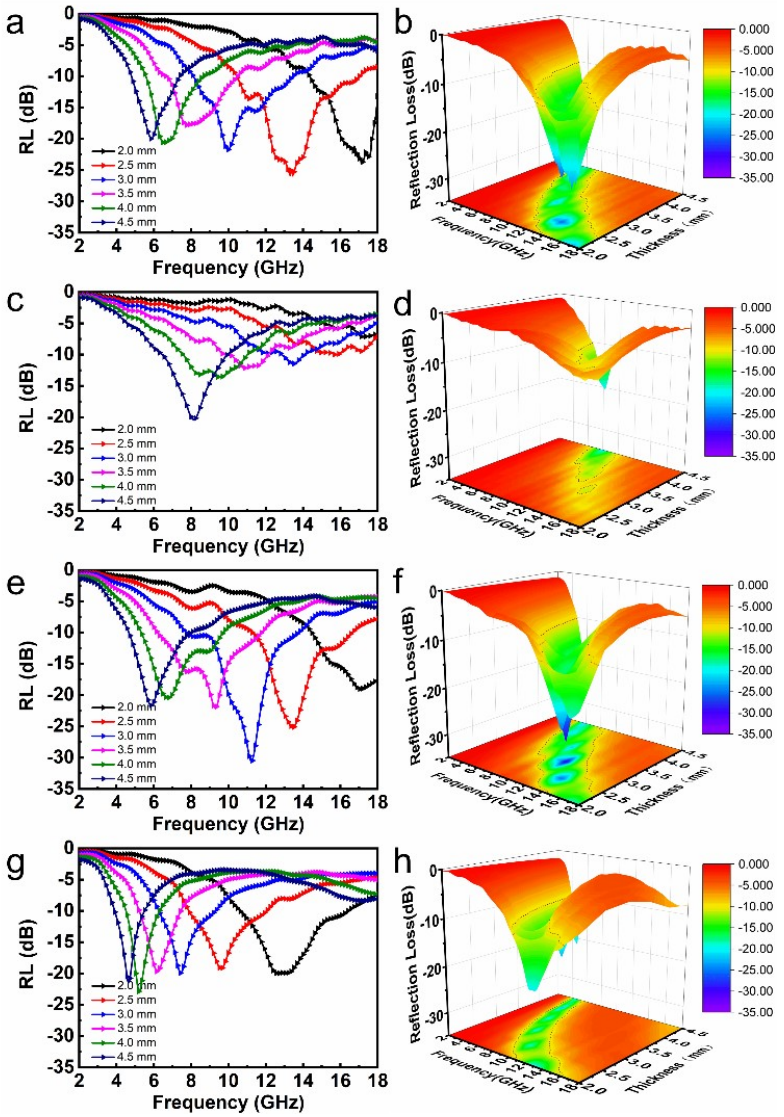

Fig.6 The RL curves, 3D RL map between thickness of 2-4.5 mm of CNF-50%(a,b), Ni/C-30%(c,d), Ni/C-50%(e,f) and Ni/C-70%(g,h)

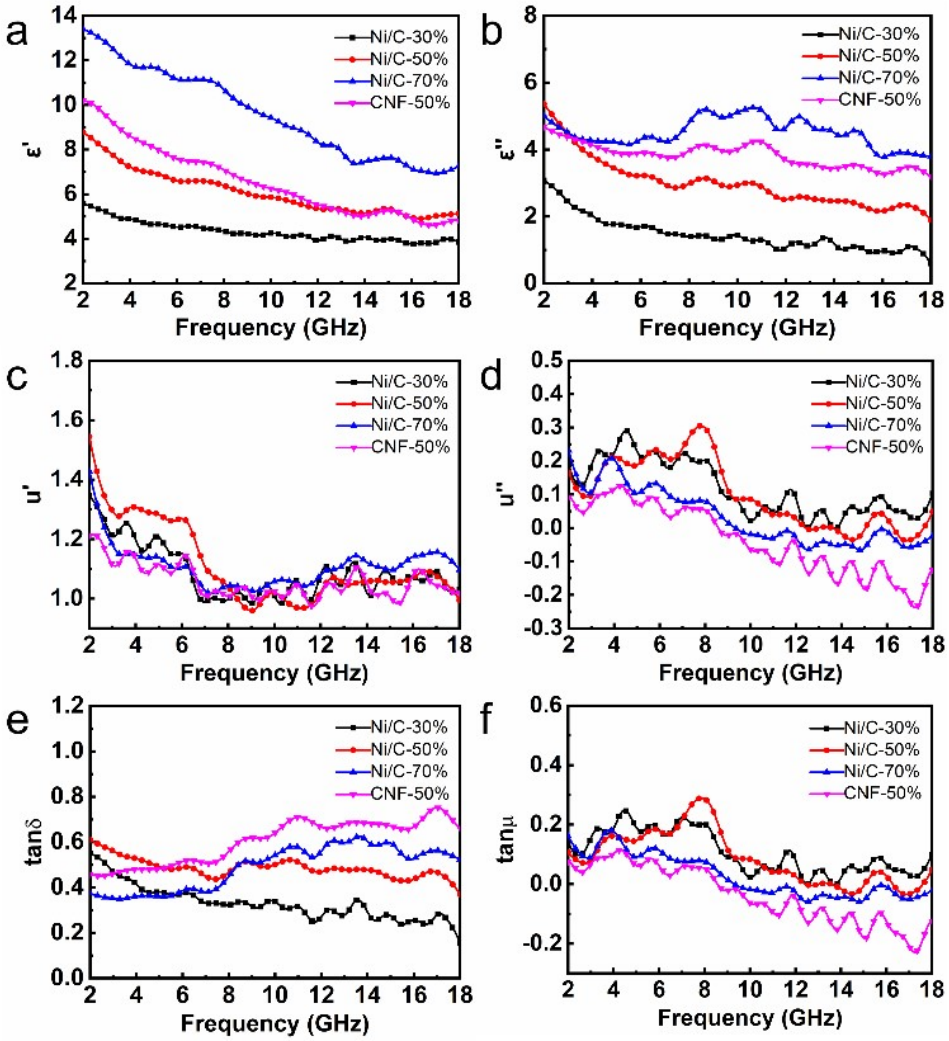

Fig. 7 Real(a) and imaginary(b) parts of complex permittivity, real(c) and imaginary(d) parts of complex permeability, dielectric loss tangents(e) and magnetic loss tangents (f) of Ni/C-30%, Ni/C-50%, Ni/C-70%, and CNF-50%

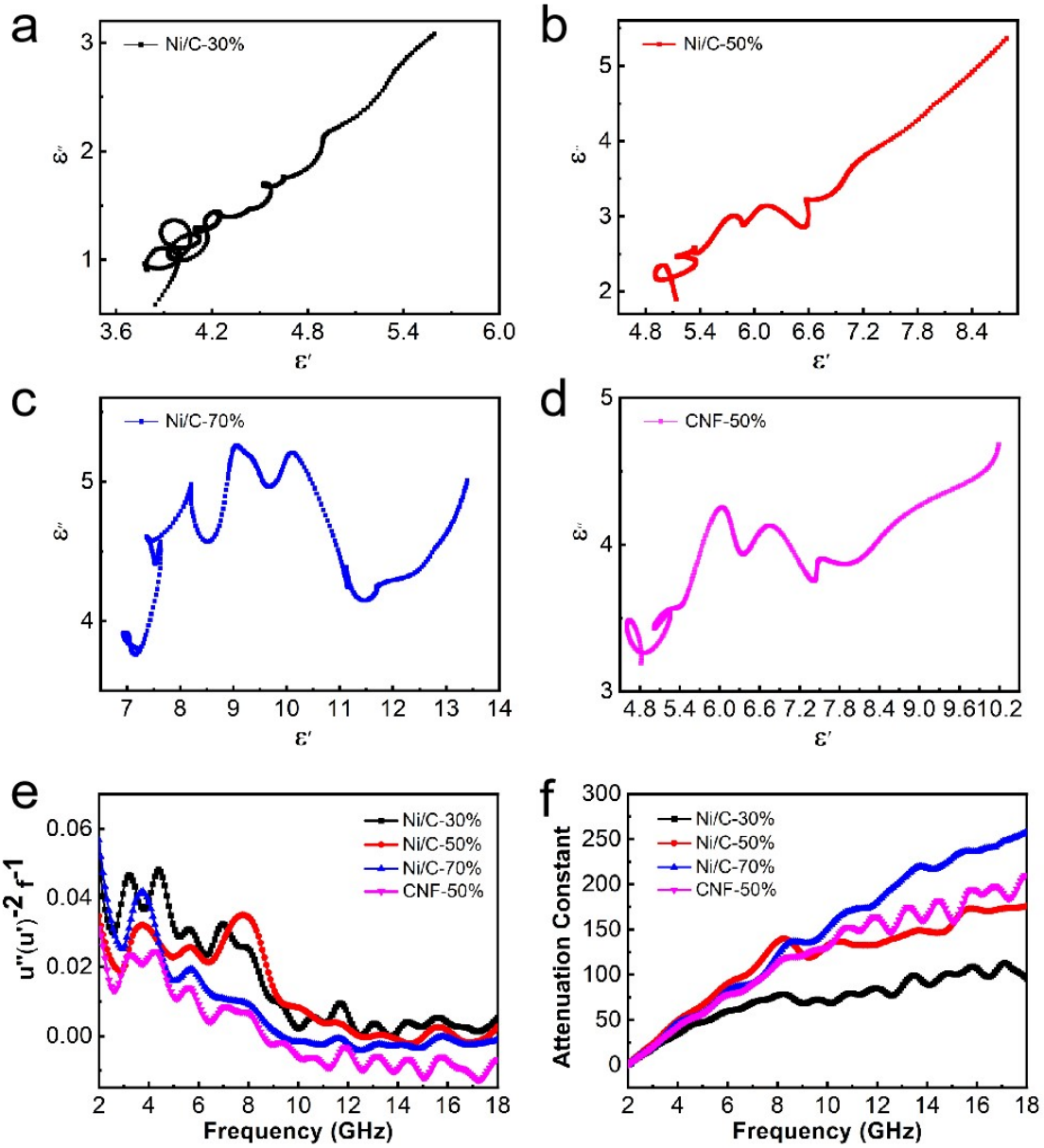

Fig. 8 Curves of $\varepsilon^{'}$ versus $\varepsilon^{''}$ (Cole–Cole semicircles) for Ni/C-30% (a), Ni/C-50% (b), Ni/C-70% (c), and CNF-50% (d). Frequency dependences of $\mu^{''}(\mu^{'})^{-2}f^{-1}$ for 30%, 50% and 70% of Ni/C nanofibers (e). attenuation constant (f) for Ni/C-30%, Ni/C-50%, Ni/C-70%, and CNF-50%

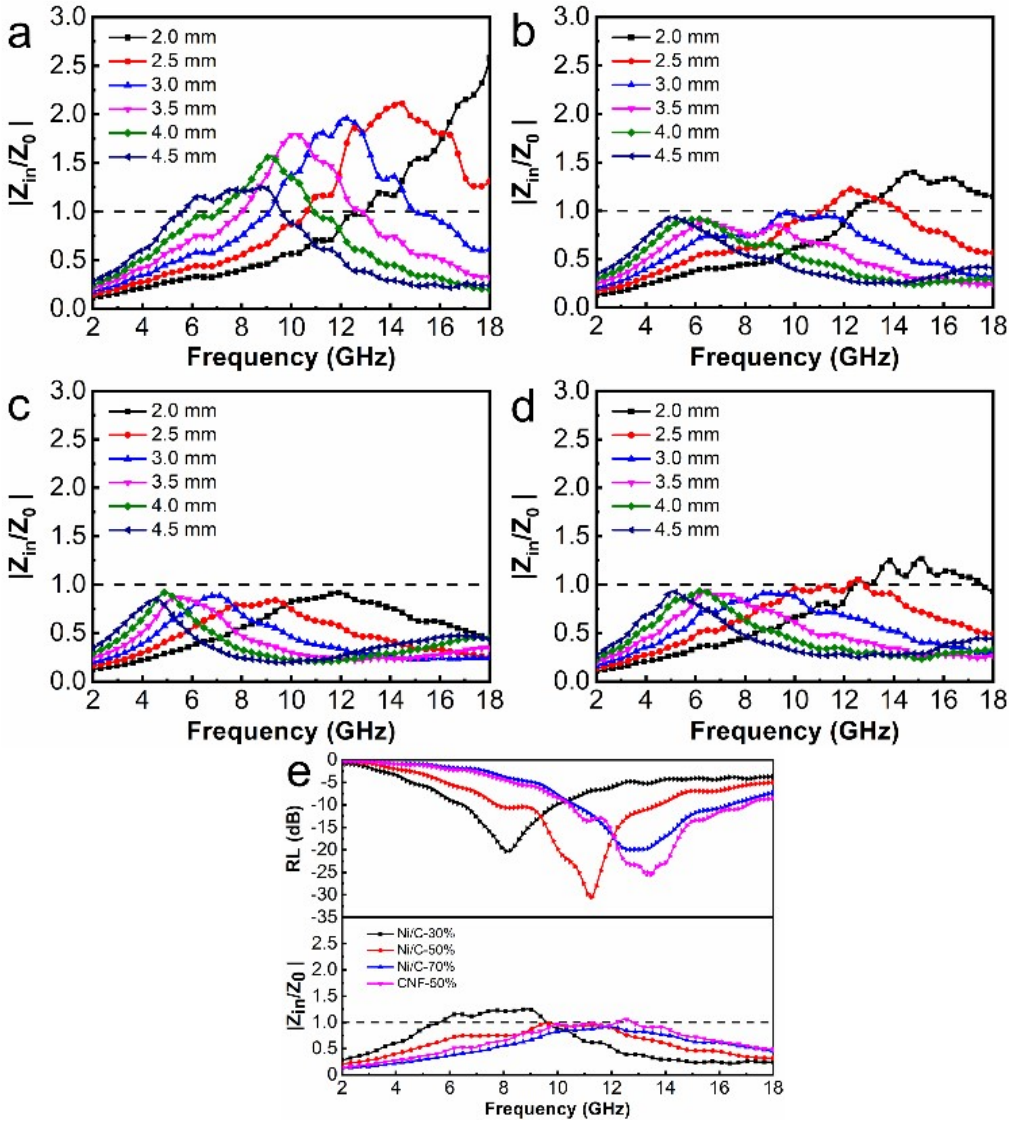

Fig. 9 The values of $|Z_{in}/Z_0|$ as a function of frequency for various thicknesses for Ni/C-30% (a), Ni/C-50% (b), Ni/C-70% (c), and CNF-50% (d). Reflection loss and impedance matching for optimal microwave absorption performance over all samples

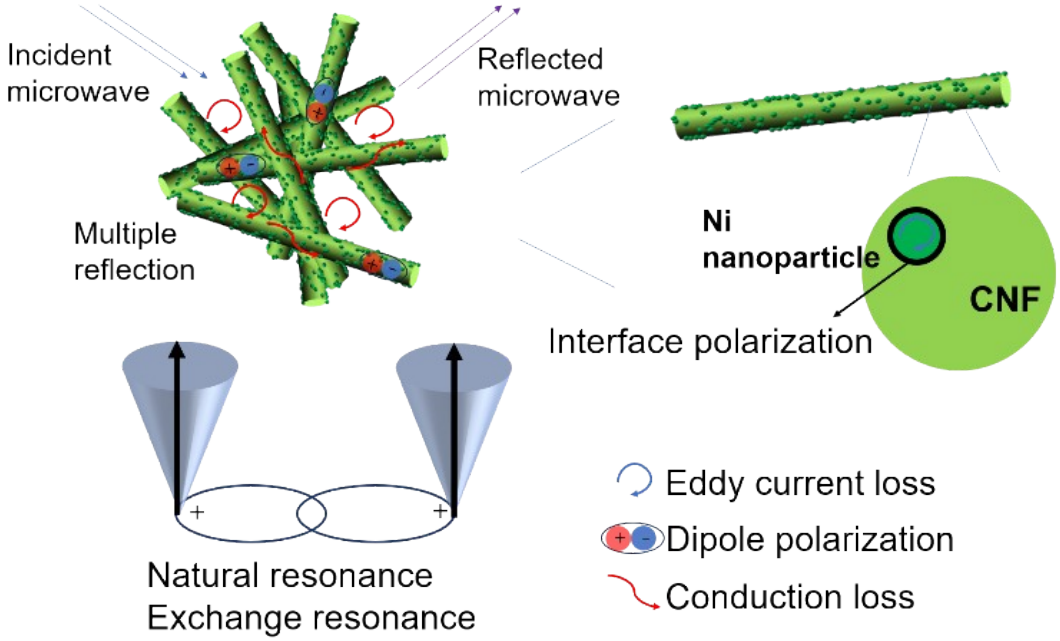

Fig.10 Microwave absorption mechanism of Ni/C nanofibers